NASA Contractor Report 159376

MODELING AND CONTROL OF TRANSONIC CRYOGENIC WIND TUNNELS: A SUMMARY REPORT

S. Balakrishna

OLD DOMINION UNIVERSITY
Norfolk, Virginia 23508

NASA Grant NSG-1503
October 1980

National Aeronautics and Space Administration

Langley Research Center
Hampton, Virginia 23665

DEPARTMENT OF MECHANICAL ENGINEERING AND MECHANICS
SCHOOL OF ENGINEERING
OLD DOMINION UNIVERSITY
NORFOLK, VIRGINIA

MODELING AND CONTROL OF TRANSONIC CRYOGENIC WIND TUNNELS: A SUMMARY REPORT

By

S. Balakrishna

Principal Investigator: G.L. Goglia

Final Report
For the period ending October 1980

Prepared for the
National Aeronautics and Space Administration
Langley Research Center
Hampton, Virginia 23665

Under
Research Grant NSG 1503
Dr. R.A. Kilgore, Technical Monitor
Subsonic Transonic Aerodynamics Division

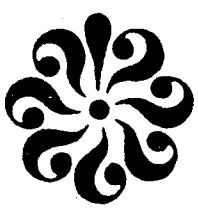

Submitted by the
Old Dominion University Research Foundation
P.O. Box 6369
Norfolk, Virginia 23508

October 1980

TABLE OF CONTENTS

LIST OF FIGURES

LIST OF FIGURES - CONCLUDED

PREFACE

This report summarizes the many faceted research activities of the project "Modeling and Control of Transonic Cryogenic Wind Tunnels," sponsored by NASA/Langley Research Center. Reported are the model synthesis activity of reference 3, control analysis activity of reference 4, test direction design analysis of reference 5, and effects of boundary-layer treatment on cryotunnel controls detailed in reference 6. The contents of references 3 to 6 are briefly reviewed, and they are complemented by recommendations for improving some of the engineering systems of the 0.3-m Transonic Cryogenic Tunnel (TCT) to which the bulk of the research was oriented.

MODELING AND CONTROL OF TRANSONIC CRYOGENIC WIND TUNNELS: A SUMMARY REPORT

By

S. Balakrishna*

INTRODUCTION

Operation of the tunnel gas of a wind tunnel at cryogenic temperatures yields considerable enhancement of flow Reynolds number. This property has been successfully exploited in realizing free flight equivalent flow Reynolds numbers on relatively small models (ref. 1). This quantum improvement in Reynolds number capability was first demonstrated by the successful operation of the 0.3-meter Transonic Cryogenic Tunnel (0.3-m TCT) (ref. 2), at NASA/Langley Research Center (LaRC) in 1974. Its success has depended on availability of bulk cryogenic liquids, cryogenic material of adequate structural properties, cryogenic instrumentation, and a candidate gas medium—nitrogen.

The initial operation of the 0.3-m TCT was by manual manipulation of the tunnel control inputs: liquid nitrogen flow into the tunnel by a valve, gaseous nitrogen flow out of the tunnel by a valve, and the fan speed. The operating experience indicated a highly coupled process which tended to creep away from equilibrium. This pointed to a need for automatic control of the cryogenic tunnel.

An investigation of the problem of automatic control of fan-driven closed-circuit, transonic, cryogenic pressure tunnels, which use gaseous nitrogen as the test medium and sprayed liquid nitrogen as the coolant, was initiated in 1978.

This document is the final summary report on this investigation and summarizes the activities on this project which have been already documented in references 3 to 6.

---

*Research Associate of Mechanical Engineering and Mechanics, Old Dominion University Research Foundation, P.O. Box 6369, Norfolk, Virginia 23508 (on leave from National Aeronautical Laboratory, Bangalore 560 017, India).

The initial aims of the investigations were to

(1) Synthesize a truly representative, control compatible, mathematical model of a cryogenic wind tunnel which describes the unsteady behavior of the tunnel, starting from basic physical laws;

(2) Validate the performance of this model by appropriate transient and quasi-steady state tests on the 0.3-m TCT and reconcile the model response to the tunnel response;

(3) Develop an understanding of the cryogenic tunnel behavior by an appropriate interactive real-time simulation of the developed model and study the cross-coupling between the various tunnel inputs and tunnel variables;

(4) Analyze the problem of closed-loop control of the tunnel states using an appropriate control theory and derive control laws for the tunnel control. These control laws were to include small error linear control and large error logic control to accommodate smoother convergence of tunnel variables for large set point commands;

(5) Translate these control laws to microprocessor-compatible flow charts and arrive at the specifications of the microprocessor controller in terms of the I/O device capability, speed of computation, accuracy of computation, uptake capability, and other associated features;

(6) Evaluate or specify the tunnel input actuators viz liquid nitrogen valve area, gas bleed valve area, and fan speed, for their accuracy, stability, and speed of response and their compatibility for desired degree of control.

(7) Evaluate and or specify the tunnel variable sensors for tunnel total pressure, tunnel total temperature, tunnel test section static pressure, tunnel fan speed, and tunnel fan power for their accuracy, speed of response, and compatibility for tunnel control.

(8) Evaluate the performance of the microprocessor-based tunnel controller while performing its function of regulating the tunnel variable states;

(9) Study the problem of test direction design in cryogenic wind tunnels so as to realize a least liquid nitrogen consumption program when associated with least dynamic pressure; and

(10) Study the effects of various types of side wall aspiration schemes, to obtain a controlled, two-dimensional flow field over the model, on the basic tunnel controls and remedies thereof.

The investigations referred to above have been performed and successfully completed over a period of 2.5 years starting in April 1978. Detailed reports on these are available as references 3 to 6. In the description which follows, a brief summary of the various activities has been provided.

MODELING A CRYOGENIC WIND TUNNEL

A literature survey at the beginning of the project in 1978 was confined to activities at NASA/LaRC since the bulk of the developmental work originated there. Further, no direct literature on cryogenic tunnel models could be expected, except as a nearly equivalent thermodynamical system. Concurrent to this project activity, efforts by the math modeling team of the National Transonic Facility at NASA/LaRC were noted.

A study of the evolution of the cryogenic wind tunnel concept (ref. 1) and its development (ref. 2) provides the physical insight into the cryogenic tunnel process. Basically, liquid nitrogen is sprayed into a pressure vessel designed as an endless aerodynamic duct. The gaseous nitrogen which is in motion in the tunnel interacts with liquid nitrogen spray and evaporates the liquid. Thermally, the motion of the gas induced by a fan generates a heating component which is intended to be cancelled by controlled inflow of liquid nitrogen. The resulting mass variation is countered by discharging a controlled mass flow rate of warmer tunnel gases out to atmosphere.

Obviously the cryogenic tunnel process is governed by physical laws such as the duct flow fluid dynamical analysis which describes motion of the nitrogen stream around the endless duct of the tunnel, including circuit losses, thermodynamical laws governing phase transition and evaporation of liquid nitrogen, including mixing, appropriate heat transfer between moving nitrogen stream and tunnel exposed material with their enthalpies, the fan mass flow-energy laws and overall mass energy conservation. A control compatible model of a cryogenic wind tunnel is the unsteady solution to the various physical laws in their entirety expressed to relate the control inputs and desired tunnel conditions.

In view of the endless nature of the duct, transit or spatial effects add to the unsteady temporal behavior of the tunnel gas. Such a process can be typically represented by distributed parameter models. Since such models are fairly complex to synthesize, various degrees of simplification can be used to derive simpler models.

In the case of National Transonic Facility modeling, the approach taken has been to solve the unsteady duct flow equations of momentum conservation, continuity, and the energy for the fluid flow, to discretize the tunnel length into a finite number of cylindrical segments, and to allow spatial effects by transport delay and appropriate design of segment boundary conditions. The model resulting from such a formulation is not explicit and can only be implicitly contained in the computer software.

In an effort to obtain an explicit model of a cryogenic tunnel in the current project, a single volume lumped model has been proposed which accounts for the total mass-energy conservation necessary to generate the model.

The first report on the project (ref. 3), "Synthesis of a Control Model for a Liquid Nitrogen Cooled, Closed-Circuit, Cryogenic Nitrogen Wind Tunnel," describes the activities on modeling of the cryogenic tunnel with emphasis on the 0.3-m TCT. This report is briefly analyzed and reviewed here.

Since nitrogen is both the medium and coolant used in a cryogenic tunnel, the thermophysical properties of element nitrogen through both the liquid and gas phase have been reviewed. In particular, nonlinear behavior of the real static gas, although behaving perfectly in isentropic expansion, and the energy involved in evaporation have been studied.

The problem of tunnel control has been analyzed using an energy state diagram. The energy state diagram (fig. 1) describes the mass internal energy relation of a finite volume of tunnel gas. The loci of constant pressure are lines roughly parallel to the mass axis with a nearly constant internal energy. The loci of constant temperature are lines radiating from the origin and having a slope of $C_v T$. If mass energy control inputs are added into such a pressure vessel, which is representative of a cryogenic pressure tunnel, the state of the gas changes as described graphically in figure 1. Fan operation introduces heat into the system and revises internal energy without mass increase, and hence is a vertical vector. Liquid nitrogen injection causes mass increase but removes heat from the gas. Hence it is a vector with

negative slope. Gas bleed causes mass reduction and energy reduction and hence is a vector of positive slope. If all the control inputs are imposed simultaneously, the vector sum of the inputs describes the way the tunnel state changes. In this analysis it is assumed that mixing is perfect, that no work is done by the gas, and the potential and kinetic energy are ignored.

The control problem has also been analytically treated using the gross thermodynamic model of a cryogenic tunnel of figure 2. In this analysis, the heat contained in the metal walls is accounted for. The tunnel mass and energy balance equations shown in figure 2 describe the basic tunnel thermodynamic process.

This simple thermodynamic balance equation obviously ignores some of the processes occurring in the tunnel viz the potential and kinetic energy of the gas, the duct flow spatial contributions, and the mechanics of liquid evaporation.

An energy content analysis is now made with specific reference to the 0.3-m TCT. Under static conditions, the enthalpy contained in the aluminum metal walls is a function of the specific heat of the metal. Reference 3 details the estimation of enthalpy in a unit mass of tunnel wall. Figure 4 illustrates the energy state diagram of the tunnel resident nitrogen which includes the metal contained energy and the gas internal energy. Figure 3 illustrates the static gas internal energy of the cryogenic tunnel. In figure 5, the kinetic energy in the tunnel stream is illustrated as a function of test section Mach number. This is independent of tunnel temperature. Figures 3, 4, and 5 can now be used to develop an understanding of the relative magnitudes of energy contained. The metal resident energy at 300 K, 6 atm is about 580 MJ. The gas internal energy at 300 K, 6 atm is about 21 MJ. The kinetic energy at M = 1 and P = 6 atm is about 200 kJ. Obviously the metal energy dominates the picture with kinetic energy being about 1 percent of internal energy and an insignificant fraction of metal stored energy.

Even if the tunnel gas were accelerated from M = 0 to M = 1 at 6 atm, the energy increment would correspond to a change of temperature of 3 K in 300 K at constant pressure. Compared to metal energy, the kinetic energy can be ignored.

Based on the above observations, the modeling of the 0.3-m TCT has been pursued as follows. The approach has consisted of determining the average dynamical state of the tunnel gas by considering the tunnel to be a thermally autonomous pressure vessel wherein ideal mixing of the mass energy control inputs occurs. This average dynamical state of the tunnel gas is superimposed on the steady-state spatial profile of the tunnel states, which in turn is obtained by the duct flow equations of continuity, momentum, and energy. Appropriate transport delay terms are superimposed on the various tunnel control inputs to account for temperature transport delay.

The results of modeling based on the above approach have led to a lumped, multivariable, nonlinear model of a cryogenic tunnel shown in figure 6. The synthesis of this nonlinear multivariable model has been exhaustively discussed in reference 3. The following features are evident from inspection of the model of figure 6.

(1) The cryogenic tunnel can be mathematically described by a three input, three output matrix model which relates the tunnel variables to the tunnel control inputs.

(2) The parameters of the tunnel matrix model are the thermophysical parameters of LN_2-GN_2, tunnel geometrical parameters like volume, length, and area, and tunnel metal and heat transfer parameters.

(3) The elements of the matrix are nonlinear functions of tunnel variables, but are dynamically linear for small perturbations.

(4) Existence of off-diagonal terms indicates dominant cross-coupling. Existence of transport delay terms points to transit effects.

(5) The model is an explicit description of the cryogenic tunnel behavior and covers the entire operation envelope of the cryogenic tunnel.

The efforts to validate the model for the 0.3-m TCT are described in the next section.

VALIDATION OF THE CRYOGENIC TUNNEL MODEL

In the case of the 0.3-m TCT, the validation of the model consisted firstly of developing a real-time, interactive, cryogenic tunnel simulator and secondly of reconciling the steady-state, quasi-steady, and transient responses of the tunnel simulator and the actual 0.3-m TCT facility.

The development of a real-time interactive simulator has been performed on a hybrid computer. The hybrid computer consists of an analogue computer, a digital computer, and a high-speed bidirectional interface between the two. In a hybrid simulation the accuracy of the digital computer and the speed of the analog computer are exploited such that nonlinear, high accuracy computations of coefficients are made on the digital computer and are communicated frequently to a continuously running analogue computer which solves the linear dynamical computations. The 0.3-m TCT model has nonlinear computations coupled with linear dynamical computations, and hence is an ideal candidate for hybrid simulation. A total digital computer simulation will not provide the interactive features of an analogue computer. A total analogue simulation cannot handle nonlinear computations accurately.

In reference 3, the hybrid computer based cryogenic tunnel simulator has been detailed fully. This facility was used to validate the tunnel model by performing quasi-steady and transient response tests as follows.

Transient Responses

The transient response study consisted of initially balancing the tunnel for equilibrium operation at a given pressure, temperature, and Mach number using the three tunnel control inputs: viz gas bleed valve area, liquid nitrogen valve area, and fan speed. Then each individual control input was disturbed by a 0.3-sec pulse of 6.25 percent valve areas or 100 rpm magnitude. The responses of the tunnel variables P, T, and M were recorded. Such transient response tests were performed firstly on the simulator and then on the 0.3-m TCT. To embrace the total envelope of tunnel operation, all combinations of pressures at 1.5 atm, 3 atm, and 5 atm, temperatures at 100 K, 200 K, and 300 K, and Mach numbers at 0.3, 0.6, and 0.75/0.9 were tried. Good agreement

between the tunnel responses and the simulator responses was found for all 27 cases. A typical response is shown in figure 7.

The individual pressure, temperature, and Mach response trajectories can also be reconciled to the math model terms. This analysis has been treated in reference 3. The main feature of this analysis is that the tunnel pressure response to liquid nitrogen input has a unique signature: when extra liquid nitrogen is injected, the tunnel pressure initially drops because of gas cooling effects. However, this cooling induces dominant heat transfer from the metal wall, thereby raising tunnel pressure. This characteristic tunnel response is unique to cryogenic tunnels with metals resident in the tunnel. Figure 7 illustrates this effect.

The tunnel and the simulator transient responses to a pulse disturbance of any input show good agreement and can be explained by basic thermodynamic laws. The absence of any oscillatory modes in the tunnel responses of temperature or Mach number point to the fact that the mixing of liquid nitrogen into tunnel stream occurs within one circuit, as was assumed initially.

In obtaining the tunnel temperature responses for the 0.3-m TCT, a type T (copper constantan) thermocouple of 0.4-mm wire diameter was used. Its response time varies with tunnel flow velocity and density around the sensor. An estimated time constant for thermocouple varies from 0.4 to 1 sec. Obviously some signal filtering of first order with 6 dB/octave does occur in this sensor.

If the tunnel temperature responses do contain circuit modes caused by recirculation of unmixed gas around the tunnel, their periods would be the same as the tunnel circuit times. The tunnel circuit time for the 0.3-m TCT varies from 0.6 to 4 sec (ref. 3). In the case of the response shown in figure 7, corresponding to 3 atm and 200 K at $M = 0.6$, the circuit time is 0.8 sec. Since the attenuation should be low, the existence of circuit modes should be obvious in figure 7 if the circuit modes did exist. The lack of circuit modes in figure 6 points to good mixing in the tunnel occurring within one circuit.

Quasi-steady Responses

Two long-term tunnel cool-down and warmup tests were performed both on the actual 0.3-m TCT and its simulator. The period involved in cool down or warmup was typically 30 to 40 min. The dominant dynamic mode in these tests was the metal heat release time constant. Figures 8 and 9 show typical cool down and warmup on the 0.3-m TCT and its simulator. The tunnel metal average temperature was sensed on the wall at an estimated point corresponding to average conditions. The cool down in figure 8 shows generally good agreement. The warmup of figure 9 shows good agreement except initially when the tunnel conditions were not proper.

An inference drawn from quasi-steady tests is that the metal stored enthalpy dictates the nitrogen consumption, since the fan energy involved in a cool down is fairly low.

Reasonably good steady-state agreement between fan speeds, valve areas, and mass flows was also found between the cryogenic tunnel and its simulator.

Thus, by comparing the transient, quasi-steady and steady-state responses of the actual tunnel and a simulator developed on the basis of the mathematical model, the model of the 0.3-m TCT of figure 6 was validated.

CONTROL LAW DESIGN AND APPLICATION

Starting from the validated multivariable model of a cryogenic tunnel, the design of a closed-loop controller for the tunnel total pressure P, total temperature T, and tunnel test section Mach number M was undertaken. The detailed design, analysis, and performance are described in reference 4.

Both a multivariable controller design and three single input/output controller designs with feed forward and gain scheduling have been considered in reference 4. By the basic thermodynamic property of the gas, the tunnel pressure and temperature loop are strongly coupled. The design of the single input/output controller for the tunnel temperature and pressure has led to design of a fan power feed forward dependent pID (proportional, integral, and derivative) control law for the temperature loop. Further, because of large static gain changes, a nonlinear gain schedule was found to be necessary which varies the temperature loop gain over a range of 1:40. Similarly the pressure loop gain required a nonlinear gain schedule of 1:10 on a pID controller, and the pressure loop did not require any feed forward.

The temperature loop gain schedule was of the form $M\sqrt{\frac{P}{T}}$, and the pressure loop gain schedule was of the form $P\frac{1}{\sqrt{T}}$. A Mach loop analysis based on varying the speed command to a fan speed control loop was found to provide good performance with a pID control law having a simple gain schedule of type $\sqrt{T}$.

The temperature and Mach loops were found to be particularly sensitive to large set errors. As such, error magnitude dependent saturation of commands had to be built in for the temperature and Mach loop. The pressure loop was found to need extra valve area, and a valve area based logic to open bias valves has been provided.

The linear control laws for the 0.3-m cryogenic tunnel temperature, pressure, and Mach number are illustrated in figures 10, 11, and 12, respectively. These loop schematic diagrams also illustrate the large error logic in the case of pressure and temperature loops. Reference 4 details the design of these loops.

At the writing of this report, the tunnel pressure and temperature control loops have been successfully mechanized on a microprocessor-based controller and commissioned. The functional flow chart for translating the control law designs into microprocessor software has been generated and provided in reference 4. The Motorola 6080 microprocessor with a 24 k memory has a floating point hardware unit and computes the combined temperature and pressure loop control laws of figures 10 and 11 in about 100 msec. The tunnel closed-loop control of the temperature and pressure has been successfully realized to a stability of ±0.25 K and ±0.017 atm. Figures 13 and 14 illustrate the tunnel performance under closed-loop control of tunnel temperature and pressure.

The fan speed loop has some speed singularities in about three speed bands. The Mach loop closure design has been completed, as detailed in reference 4, but has yet to be implemented.

The design of the single input/output controller has proven to be adequate. Though a multivariable controller has been designed, as in reference 4, it has not been implemented.

TEST DIRECTION DESIGN IN CRYOGENIC TUNNELS

Having achieved the ability to operate the cryogenic tunnel at any given tunnel total pressure and temperature at various fan speeds, the question of deciding the desired pressure and temperature arises.

The goal of a wind-tunnel test is to generate the flow characteristics of a model as a function of certain flow parameters, viz Mach number, Reynolds number, angle of attack and sometimes flow dynamic pressure. Thus a wind-tunnel test program is initially conceived as one of generating desired flow parameter combinations. In ambient temperature tunnels, Mach number was the only true flow parameter that could be varied to maintain flow similarity between the model and its full-scale prototype. The cryogenic tunnel concept has created the ability to maintain flow similarity in respect to both Mach number and Reynolds number.

The problem of a cryogenic tunnel test design can be defined as one of translating the desired Reynolds number-Mach number combinations into the tunnel flow variables, viz total pressure and total temperature at given Mach number, subject to some constraint. Since a given combination of Re-M can be generated by a set of P-T combinations, an optimizing P-T combination should be chosen to yield an extremum in a performance index. The performance index can be minimum consumption of liquid nitrogen or minimum dynamic pressure.

This problem has been treated exhaustively in reference 5. The main result of this analysis in reference 5 is that there is a minimum nitrogen consumption locus in the P-T plane which can generate all tunnel flow parameter combination of Re and M. This locus is not only capable of providing minimum energy consumption, but also is the minimum dynamic pressure locus. The locus is the minimal pressure-temperature line till the saturation line is encountered, and then it is the safe vapor phase line at any pressure. This locus is illustrated in figure 15.

Thus, given a test program in Re-M combinations, the best choice of P-T can be determined with the order in which the tests should be performed. Figure 15 summarizes the test direction design problem and

its solution. A computer program which performs the test direction design has been detailed in reference 5.

EFFECTS OF BOUNDARY-LAYER TREATMENT SCHEMES ON CRYOGENIC TUNNEL CONTROLS

In any two-dimensional wind-tunnel test section, the flow field over the airfoil model is sensitively controlled by the side wall boundary-layer growth. To generate good data from the wind tunnel, it may be necessary to control this boundary-layer growth by some form of boundary-layer treatment. One of the techniques of obtaining a good two-dimensional flow field over a model is to aspirate the side wall and create a mass flow across to control boundary-layer growth.

In a cryogenic wind tunnel, any efforts at aspirating mass flow of the test section are likely to upset the thermodynamic balance of the tunnel. This aspirated mass flow can be passively discharged out of the tunnel, but it then creates a mass unbalance. Alternatively, the aspirated mass flow can be reinjected using a fan/compressor. This scheme does not create a mass unbalance, but creates an energy unbalance due to compression heating.

If a cryogenic tunnel is to maintain its thermodynamic equilibrium, it is necessary to make up mass or energy appropriately. Whether this can be handled by the control laws discussed previously has been addressed in reference 6. This document considers two schemes of passive bleed boundary-layer treatment wherein the mass unbalance is made up by either gaseous nitrogen makeup or liquid nitrogen makeup. The analysis of the system indicates that the control laws generated for tunnel control are adequate only as long as mass makeup and energy contained exceed an estimated magnitude. In the case of liquid makeup, need for an electrical heater is indicated.

Reference 6 also considers two schemes of reinjection: total boundary-layer bleed reinjection and a partial reinjection. The energy unbalance created by the reinjection schemes can be easily handled by the tunnel control laws as disturbances.

Relative merits of the four schemes of side wall boundary-layer treatment are detailed in reference 6. The reinjection scheme is energy efficient if a good fan can be designed to work within the surge boundary, but tends to be equipment intensive. The liquid makeup

heater scheme is the simplest but not very energy efficient. In reference 6, the effects of boundary-layer treatment schemes involving mass aspiration on the tunnel controls are considered. The need to maintain the mass-energy balance of the tunnel is established.

ENGINEERING SYSTEMS OF 0.3-m TCT

The control of the 0.3-m TCT can be achieved only through the chain of control input actuators, tunnel variable sensors, and the tunnel controller. The control stability and accuracy depend entirely on all the elements of this chain. Hitherto discussion was confined to the math model and the controller design. These have been discussed in reference 4 in detail. The performance of the other elements of the tunnel is now reviewed.

Fan Drive

The 0.3-m TCT fan is driven by a 2-pole water-cooled induction motor driven from a variable frequency electrical source capable of generating 3 to 120 Hz and maintaining a constant voltage/frequency ratio of 35 V/Hz. This speed control stability and accuracy are achieved by a Kramer type speed control of rotating machines. One of the initial problems resolved in the project was modeling of the speed control system dynamics. This was achieved by analyzing the speed records of the tunnel using modern identification procedures detailed in Appendix A. This appendix deals with autoregressive modeling of the fan speed records while running under nominal steady-state conditions. The model realized has been used for all control analyses in references 3 and 4.

Another problem of this speed control system is the existence of speed bands at which the tunnel fan cannot be run. These are at 1,000, 3,500 to 3,700, and 4,800-5,200 rpm. Such speed singularities cause a void in the capability of the 0.3-m TCT.

In order to overcome such a problem, a new speed control system for tunnel fan has been proposed in Appendix B, and consists of a solid-state cycloconverter drive capable of generating the required variable frequency electrical power.

Liquid Nitrogen Source

The mass flow control of the liquid nitrogen into the 0.3-m TCT is through area control of a valve with the source being a high-pressure liquid nitrogen line. The existing liquid nitrogen pumping system is a

positive displacement pumping system with a relief valve. Since liquid nitrogen is incompressible, this pumping system has a hard pressure control and demonstrates violent pressure fluctuations for flow and drive disturbances. Numerous tests were performed to test the liquid nitrogen system. Results of the tests can be summarized as follows:

(1) The existing liquid nitrogen pumping system with its relief control valve can maintain pressure between 3 to 10 atm under steady flow conditions.

(2) The supply line loop is about 50-m long and any flow disturbances cause pressure fluctuations and occasionally create cavitation at 20 Hz.

(3) The relief control using pI tuning is adequate for steady operation.

(4) Under low reservoir volume conditions with thermal leakage in the suction line, two-phase flow in the pump occurs occasionally and makes pressure buildup difficult. This can be remedied by increasing static head and by improved insulation on the suction side.

The problem of pressure fluctuations which occur when flow demand into the tunnel varies, as is the case under closed-loop temperature control, can be simply overcome by a gas-liquid accumalator to accommodate incompressibility effects of the fluid.

Inclusion of a gas accumulator in the liquid nitrogen system is recommended. A bag accumulator cannot be had because of material problems. Either a piston type accumulator with a gas like helium or a nitrogen gas accumulator is recommended.

A 37.9- to 75.7-liter (10- to 20-gal) volume upright accumulator to be located near the tunnel can be designed as follows. The accumulator is fully insulated with a heater on the metal wall. The heater energy is controlled such that the top half of the upright tube is full of nitrogen gas and the bottom half is exposed to the liquid line. This volume of gas can buffer the pressure fluctuations. Without heat the liquid is likely to dissolve the gas into itself. By proper control of the liquid gas surface in the accumulator, the system pressure can be stabilized very well.

In summary, the two problems of the existing liquid nitrogen system, viz two-phase flow and pressure fluctuations, can be overcome by improving the suction leg of the pump thermally and the liquid head, and by introduction of a gas accumulator which renders the system soft. With these improvements the tunnel controls can function much better and smoother.

Liquid and Gas Flow Actuators

The tunnel mass control is by area manipulation of the inlet liquid flow and bleed gaseous flow. Originally, 2 digital valves with 10-bit and 8-bit resolution were used to control the area (ref. 4). These valves had fine resolution under steady-state conditions used manually, and this feature allowed fine tuning of area.

Under closed-loop operation, the control laws create continuously varying areas all the time. This fast updating creates fatigue problems on the digital valves.

As an alternative, use of electrohydraulically actuated globe valves is recommended for gas valves. In view of the continously varying command from the controller, the valve needs to have one- to two-Hz response, and to possess adequate life. Electrohydraulic actuators are known to have lives up to 20 years with adequate maintenance. Such a valve was developed for the 0.3-m TCT and commissioned. Such a valve has been used for the pressure loop successfully.

CONCLUDING REMARKS

The project under research grant NSG 1503, "Modeling and Control of Transonic Cryogenic Tunnels," which was undertaken with specific emphasis on the 0.3-meter Transonic Cryogenic Tunnel test facility at NASA/LaRC, has realized all the initially set goals detailed in the introduction. This activity has resulted in a validated control model of the liquid nitrogen cooled, gaseous nitrogen, cryogenic pressure tunnel, in general, and 0.3-m TCT specifically. In order to validate the model, a real-time interactive hybrid simulator has been developed for the 0.3-m TCT. This simulator is capable of assisting in operator training and provides a mathematical analogue of the tunnel. Using this validated model, which agrees with the 0.3-m TCT for transient, quasi-steady and steady-state responses, closed-loop control laws for tunnel pressure, temperature, and Mach number have been generated. These control laws have been translated to a microprocessor-based controller for the 0.3-m TCT tunnel pressure and temperature. The controller has been successfully commissioned to realize ±0.25 K in temperature and ±0.017 atm in pressure. Recommendations have been made for engineering improvements to the liquid nitrogen pumping system, the tunnel mass flow control valves, and the fan speed control system.

Further, use of the tunnel controls to realize minimum energy consumption test programs has been proposed to provide optimal test direction design. This strategy can save considerable amounts of energy. Also considered have been the effects of modifications, made to the tunnel to realize boundary-layer treatment on the basic tunnel controls.

In conclusion, the spectrum of problems associated with control of cryogenic tunnels has been successfully solved at the analytical and experimental levels. These have been fully documented in this report and complemented by references 3 to 6.

ACKNOWLEDGMENTS

The author wishes to express his gratitude and appreciation to the following persons from NASA/LaRC for their contributions to the present research effort:

- Dr. R.A. Kilgore for his direction and encouragement;
- Mr. Jerry J. Thibodeaux for his continuous cooperation, participation, and discussions; and
- Mr. J.B. Adcock, Mr. P.L. Lawing, Mr. C.B. Johnson, Mr. E.J. Ray and Mr. C.L. Ladson for their data inputs and discussions.

Further the author wishes to record his appreciation for the guidance he received from Dr. G.L. Goglia, Professor and Chairperson, Department of Mechanical Engineering and Mechanics, Old Dominion University. The author also wishes to acknowledge the excellent support he received from the personnel of Old Dominion University Research Foundation, particularly the contributions of Publications Coordinator, Ms. M.A. Lippman, Technical Typist, Ms. C.B. Speller and the Editor, Ms. A. Tennille.

APPENDIX A

FAN SPEED DYNAMICS

The fan speeed control system consists of a rotating variable frequency generating system, generating a 30 V a.c./Hz electrical supply which drives the 0.3-m TCT fan through a 2-pole induction motor. The dynamics of this system consist of the fan load, fan inertia, induction motor, rotating machinery inertia and its dynamics, and the speed control system controller. Modeling such a system is quite complex.

In the approach used here, an autoregressive modeling approach is used. The basis for autoregressive modeling is as follows. Any linear dynamical system, when exposed to white noise perturbation which is inaccessible, generates an output spectrum which is characteristically the system dynamics. The tunnel fan speed, while maintained nominally constant, still is disturbed by noise processes in the system. Typically for the 0.3-m TCT, this ranges between about 5 to 10 rpm. By analyzing this record of fan speed on the following basis, the fan dynamics can be obtained.

Modeling

The nominal steady-state fan speed is taken to be that of an nth order linear dynamical system, the fan dynamics excited by an inaccessible white noise. This noise is assumed to be stationary over the period of observation. This continuous random process, defined as $\{y(t)\}$, is observed as a discrete random process $\{y(k)\}$, $k = [0,1,\ldots n+N]\Delta t$ where $N \gg n$, using uniformly spaced samples taken at intervals Δt by a zero order sampler. The sampling interval is chosen to be compatible with the spectrum of interest (ref. 7). Then

$$e(k) = A(z^{-1})y\ (k) \tag{1}$$

represents an autoregressive process, where

z^{-1} = backshift operator representing sampling time

$A(z^{-1})$ = mathematical model of the fan dynamics

$= 1 + a_1 z^{-1} + a_2 z^{-1} + \ldots a_n z^{-n}$

$e(k)$ = independently and identically distributed white noise

Equation (1) can be rewritten in the prediction form as

$$y(k) = e(k) - [a_1 y(k-1) + a_2 y(k-2) + \ldots a_n y(k-n)] \qquad (2)$$

The significance of autoregressive modeling is that the output of the model is dominantly a function of its previous history over a period $n\Delta t$, with an additive but inaccessible noise.

Equation (2) can be rewritten with $e(k)$ replaced by $r(k)$ to represent residuals in the estimation procedure as

$$y(k) = r(k) - [a_1 y(k-1) + a_2 y(k-2) + \ldots a_n y(k-n)] \qquad (3)$$

If N such observations are made consecutively, the set of such observations can be expressed in the vector matrix notation as

$$\underline{Y} = B\,\underline{\lambda} + R \qquad (4)$$

where

$$\underline{Y} = [y(n+1),\ y(n+2)\ \ldots\ y(n+N)]^T$$

$$\underline{\lambda} = [-a_1\ -a_2\ \ldots\ -a_n]^T$$

$$B = \begin{bmatrix} y(n) & y(n-1) & \ldots & y(1) \\ y(n+1) & y(n) & \ldots & y(2) \\ y(n+N-1) & \ldots & \ldots & y(N) \end{bmatrix}$$

The parameter vector $\underline{\lambda}$ can be evaluated by minimizing the loss function V_n:

$$V_n \triangleq \frac{1}{2} \sum_{k=1}^{N} r^2(k)$$

$$\hat{\lambda} = (B^T B)^{-1} B^T \underline{Y} + (B^T B)^{-1} B^T \underline{R} \qquad (5)$$

with the assumption that residuals represent inaccessible zero mean white noise, the second term of the equation tends to zero, for large observation vector length N. Consequently r(k) = e(k) and

$$\hat{\lambda} = (B^T B)^{-1} B^T \underline{Y}$$

In this process model, order n should be determined using some performance index.

Estimation of Fan Dynamics

Records of steady-state runs from test 106 of the 0.3-m TCT were used in the present analysis. The test 106, which was meant for pressure calibration, consisted of runs 50 to 58 which covered a pressure range of 1.2 to 5 atm, temperature range of 100 to 300 K and Mach number range of 0.3 to 0.87. Typically records over a period of 150 sec, the time taken for one scanivalve scan were available, which were sampled at about 1.02 sec.

Using these chains of data, autoregressive analysis was performed. Firstly a number of model dimensions ranging from 3 to 6 were tried. For a typical run, the performance index as a function of model order was as follows:

n	Performance Index $\sum r^2(k) \frac{N+h}{N-n}$
3	1954
4	1926
5	1811
6	1829
7	1857

This suggests a model order of 5. Subsequent analysis was confined to model order of 5.

The roots of the polynomial

$$1 + a_1 z^{-1} + a_2 z^{-2} + \ldots + a_5 z^{-5} = 0 \qquad (6)$$

were determined. Characteristically all these roots fall within the unit circle diameter of one for a physically realizable system. The complex magnitudes of the roots are indicative of the system dynamics.

Nearly 50 records of runs 50 to 58 of test 106 were analyzed, and the fifth order autoregressive coefficients were determined. The coefficients were translated into system eigenvalues by determining the roots of the coefficient polynomial of equation (6).

Typically the average root system of the 50 records was

$$z^{-1} = 0.98$$

$$z^{-1} = -0.52 \pm i\ 0.48 \qquad i = \sqrt{-1}$$

$$z^{-1} = 0.68 \pm i\ 0.05 \qquad i = \sqrt{-1}$$

The first root is indicative of the integration occurring in the data. The second conjugate pole pair represents the system dynamics. After allowing for variance, the system could be approximated, for all the 50 records, to

$$\frac{1}{0.2\ S^2 + 0.56\ S + 1}$$

The third conjugate pole pair is almost a negative real root which can be ignored, since it is caused by quantization. Thus the typical dynamic response of the fan speed system to a small perturbation is a simple second order response. This response embraces the total chain including the tunnel load.

APPENDIX B

SPEED CONTROL SYSTEM SPECIFICATIONS

In view of certain shortcomings of the existing speed control system, in particular the nonoperable speed bands, a new solid-state, variable frequency generator is conceived. Following are the typical specifications of a variable frequency generator, which can directly drive the existing two-pole, water-cooled, induction motor.

Specifications

Motor:

(1)	Type of electrical motor:	2-pole, a.c., squirrel cage, induction motor
(2)	Rated maximum power:	2240 kW
(3)	Number of poles:	2
(4)	Rated maximum speed:	7178 rpm at full slip (7200 rpm synchronous)
(5)	Supply:	3-phase a.c., 4250 V rms between phases, at 120 Hz for full speed
(6)	Variable speed operation:	Maintain 35.5 V rms/Hz
(7)	Current:	420 A maximum
(8)	Type of cooling:	Water cooled, full enclosed
(9)	Temperature rise:	80° C continuous 100 ° C for 0.5 hr
(10)	Mounting:	Type CS

Load:

The motor drives a cryogenic tunnel fan of the following particulars:

(1)	Fan details:	12-blade rotor with 7 guide vanes
(2)	Fan speed torque characteristics at steady-state:	$\text{Power} = 111 \frac{P}{\sqrt{T}} \left[\frac{N}{1000}\right]^{2.6}$ kW $\text{Speed} = 597\ M\sqrt{T}\ (1-0.3\ M)\ P^{-0.035}$

Valid for $300 \leq N \leq 5600$, fan speed

$80\ K \leq T \leq 350\ K$, tunnel gas temperature

$1\ atm \leq P \leq 6\ atm$, tunnel pressure

(3) Maximum fan power: 1800 kW at 5600 rpm

The load speed torque characteristics and speed power characteristics are given in figures 16, 17, 18, and 19 for gas temperatures of 100 and 300 K.

Speed Control:

It is desired to obtain a solid-state, Thyristor-controlled, speed control system to drive the fan load using the existing motor which should perform to following specifications:

(1)	Speed control type:	d.c. Link, Thyristor synthesized, variable frequency generator having an e/f capability of 35 V/Hz
(2)	Range of speed control:	300 to 7200 rpm (1:24)
(3)	Accuracy of speed:	±5 rpm of set value
(4)	Stability of speed control:	±3 rpm of set value
(5)	Load acceleration:	300 rpm/sec anywhere
(6)	Speed control bandwidth:	4 rad/sec and 0.6 damping
(7)	Speed sensor:	Toothed wheel pulse counter available
(8)	Overall performance:	The fan load has been designed to operate away from surge. The speed stability to be demonstrated for typical flow induced rpm instabilities
(9)	Remote control:	0-5 VDC analog command for full range to be allowed from remote stations
(10)	Environmental effects:	The Thyristor switching circuit should not induce electrical radiation or line noise.
		Radiation = 20 V/m at 1 kHz, at 2 m
		Line noise: less than 1 percent ripple

The d.c. link speed control system detailed above will be able to provide continuous control of tunnel conditions.

REFERENCES

1. Kilgore, R.A.; Goodyer, M.J.; Adcock, J.B.; and Davenport, E.E: The Cryogenic Wind Tunnel Concept for High Reynolds Number Testing. NASA TN D-7762, Nov. 1974.

2. Kilgore, R.A.: Design Features and Operational Characteristics of the 0.3-m Transonic Cryogenic Tunnel. NASA TN D-8304. Dec. 1976.

3. Balakrishna, S.: Synthesis of a Control Model for a Liquid Nitrogen Cooled, Closed-Circuit, Cryogenic Nitrogen Wind Tunnel and Its Validation. NASA CR-162508, Nov. 1979.

4. Balakrishna, S.: Automatic Control of a Liquid Nitrogen Cooled, Closed-Circuit, Cryogenic Pressure Tunnel. NASA CR-162636, March 1980.

5. Balakrishna, S.: Minimum Energy Test Direction Design in the Control of Cryogenic Tunnels. Progress Report for NASA grant NSG 1503, NASA CR-163244, June 1980.

6. Balakrishna, S.: Effects of Boundary Layer Treatment on Cryogenic Wind Tunnel Controls. Progress Report for NASA grant NSG 1503, NASA CR-159372, August 1980.

7. Balakrishna, S.; and Jategaonkar, R.V.: Autoregressive Modeling and Damping Evaluation from Random Excitation Response of Structures. Proceedings of National Systems Conference, paper B-1, held at Coimbatore, India, 1977.

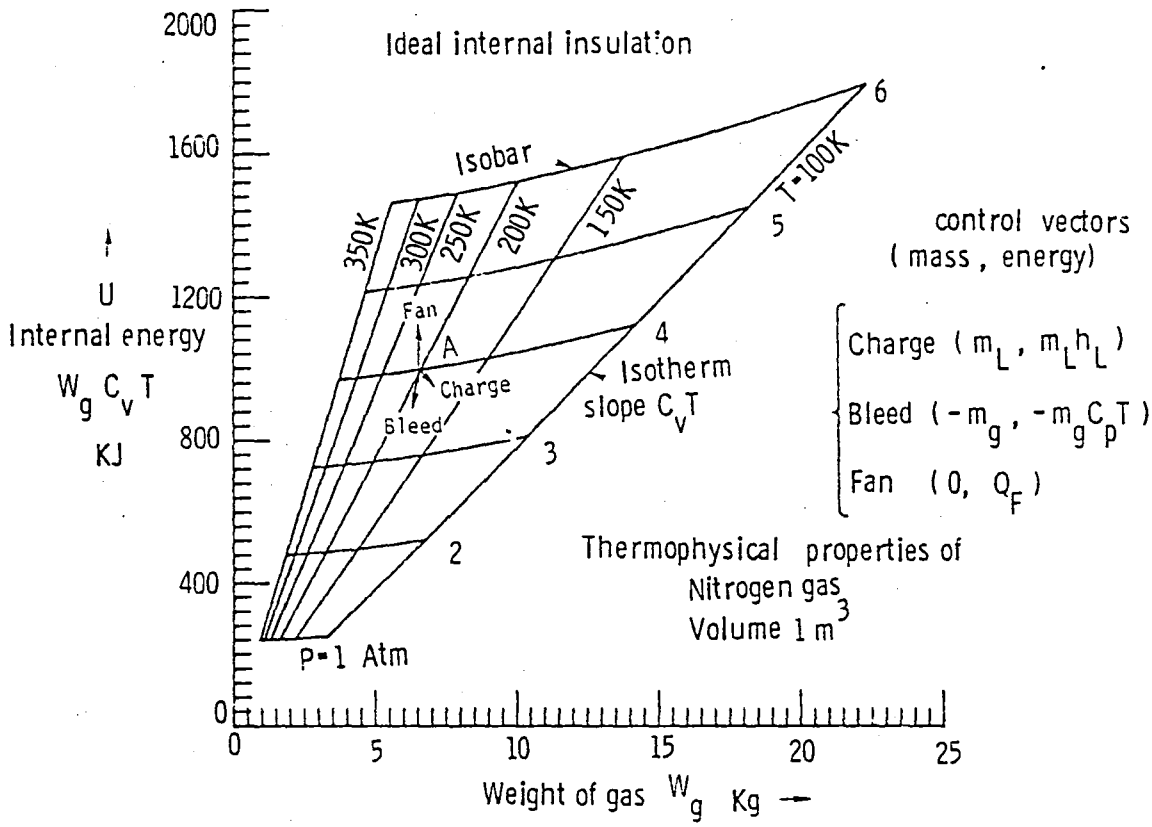

Figure 1. Energy state diagram.

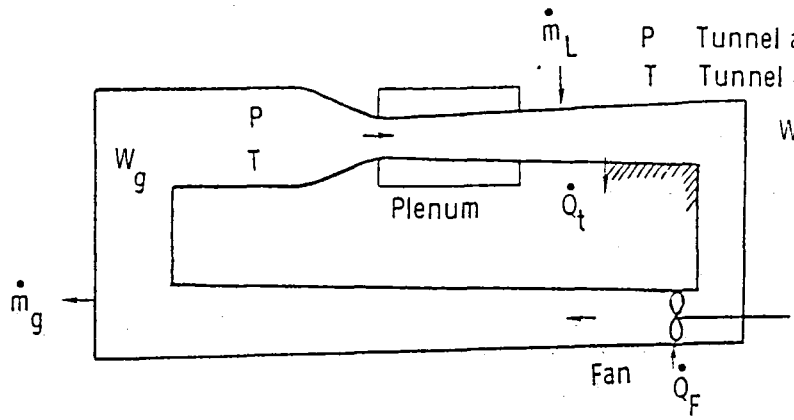

P Tunnel average pressure, atm

T Tunnel average temperature, K

W_g Mass of tunnel gas, kg

Assumptions

Perfect gas behavior
Uniform tunnel temperature
Work, potential & kinetic energy ignored

first law of thermodynamics $$-\dot{Q}_t + \dot{Q}_F + \dot{m}_L h_L - \dot{m}_g h_g = W_g C_v \frac{dT}{dt} + u(\dot{m}_L - \dot{m}_g)$$

Where

h_L Liquid nitrogen enthalpy J/kg

u Specific internal energy

h_g Gas enthalpy J/kg

$\dot{Q}_t$ Heat flow from tunnel metal wall J/sec

$\dot{Q}_F$ Heat flow from Fan operation J/sec

$\dot{m}_g$ Gaseous nitrogen bleed kg/sec

$\dot{m}_L$ Liquid nitrogen mass flow kg/sec

Figure 2. Thermodynamic model of a cryogenic tunnel.

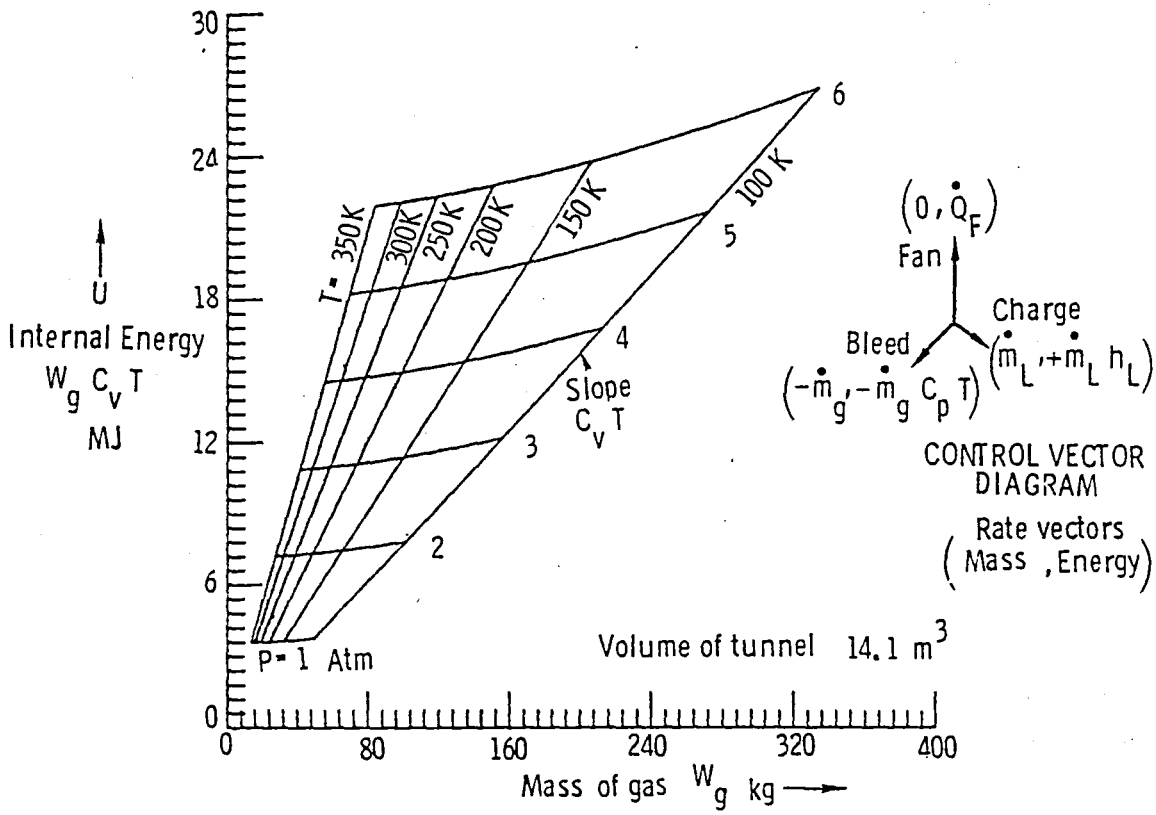

Figure 3. Energy state diagram including metal enthalpy of 0.3-m TCT.

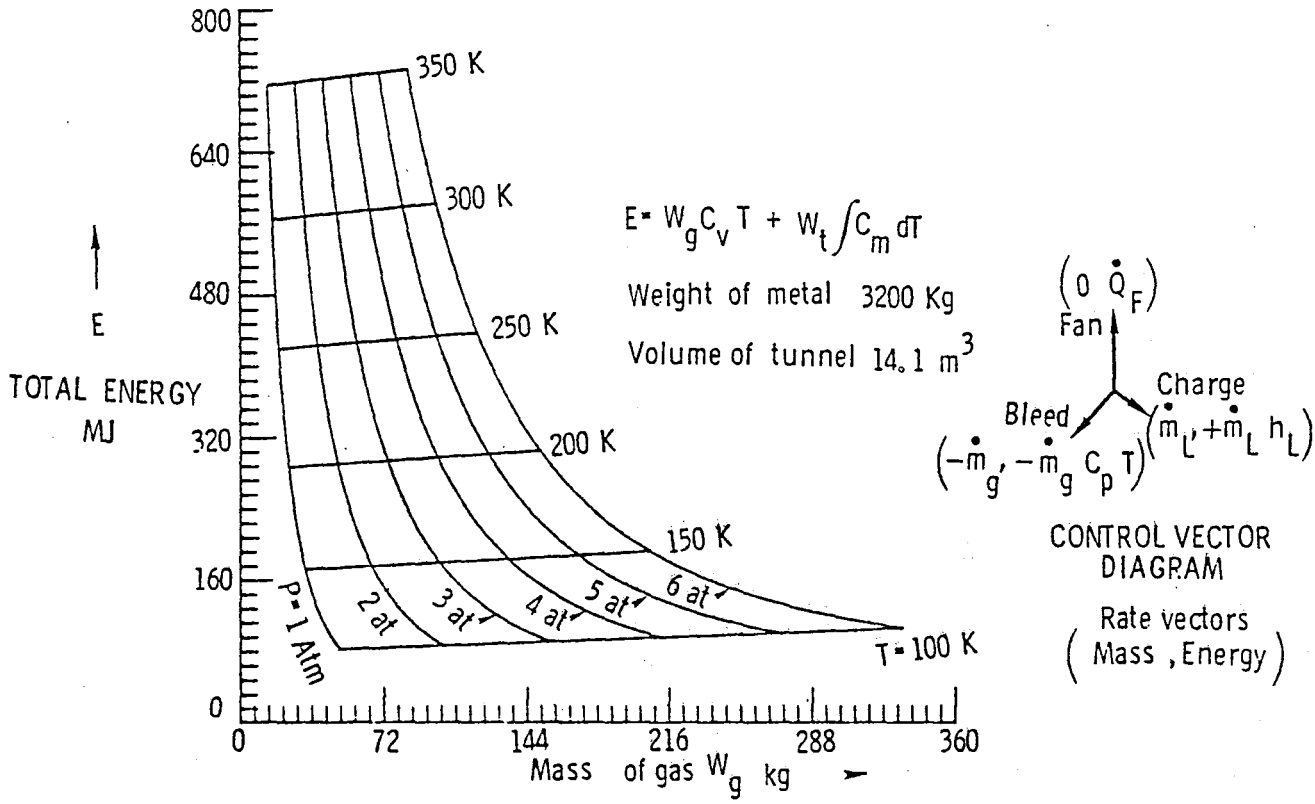

Figure 4. Energy state diagram of gas, 0.3-m TCT.

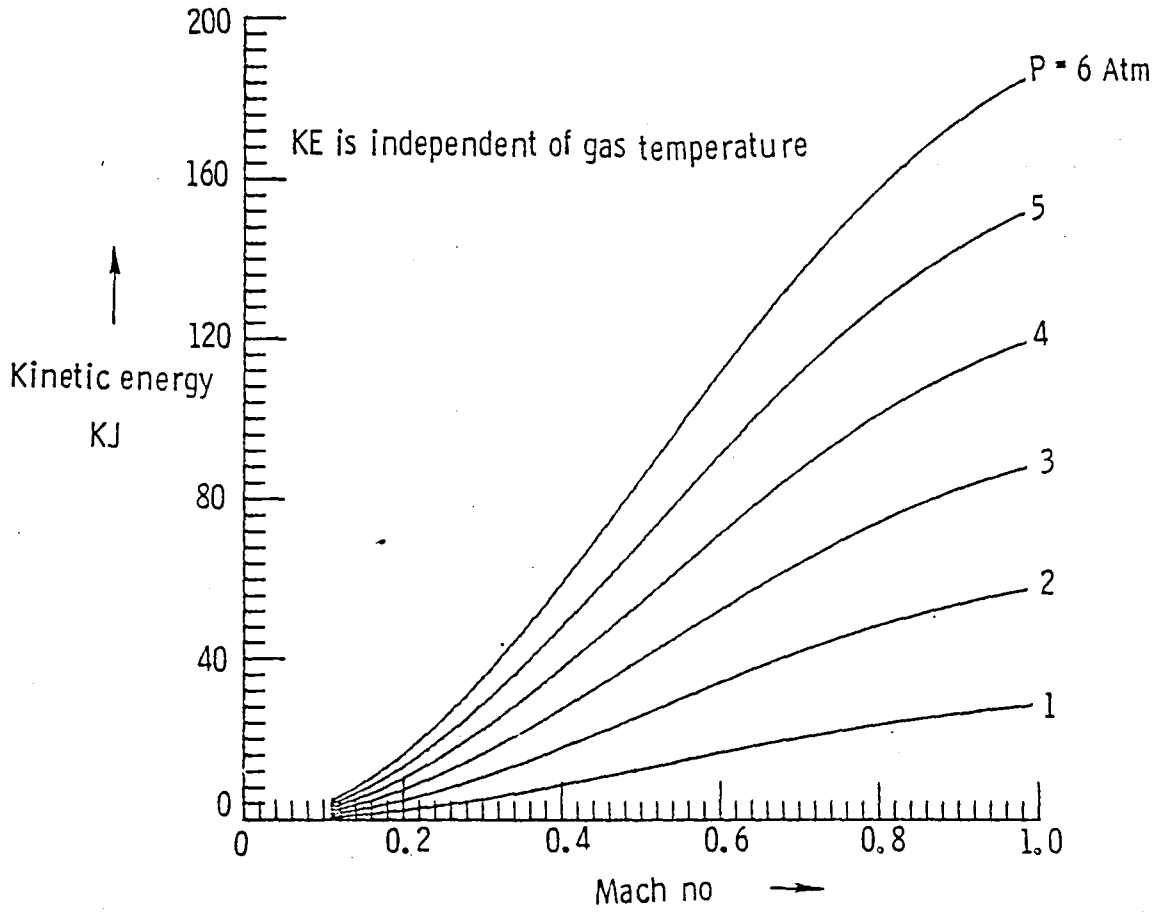

Figure 5. Kinetic energy of nitrogen stream in 0.3-m TCT.

TUNNEL PROCESS MODEL

$$\begin{bmatrix} o_T \\ M \\ o_P \end{bmatrix} = \begin{bmatrix} k_L \cdot \frac{\beta+\alpha}{\theta} \cdot \frac{1+t_m s}{1+t_g s} e^{-\tau_L s} & \frac{k_f}{k_m} \cdot \frac{PM^2}{\theta(1+0.2M^2)^3} \cdot \frac{1+t_m s}{1+t_g s} e^{-\tau_f s} & -k_g \frac{Pa}{\sqrt{T\theta}} \frac{1+t_m s}{1+t_g s} \\ 0 & \frac{e^{-\tau_a s}}{k_m \sqrt{T\eta}\,(1+t_p s)} & 0 \\ k_L \left[\frac{P}{W_g} + \frac{P(\beta+\alpha)}{T\theta} \frac{1+t_m s}{1+t_g s}\right] & \left| \frac{k_f}{k_m} \cdot \frac{P^2M^2}{T\theta(1+0.2M^2)^3} \cdot \frac{1+t_m s}{1+t_g s} + \frac{bMPs}{k_m\sqrt{T}} \right| & -\frac{k_g P}{\sqrt{T}} \left[\frac{P}{W_g} + \frac{Pa}{T\theta} \cdot \frac{1+t_m s}{1+t_g s}\right] \end{bmatrix} \times \begin{bmatrix} A_L \\ N \\ A_g \end{bmatrix}$$

Figure 6. Multivariable mathematical mode of cryogenic tunnel.

ACTUATORS AND SENSOR MODELS

LN_2 VALVE - $\dot{m}_L = k_L A_L = 3.47 \sqrt{P_L - P}\ A_L$ $\quad 0 \le A_L \le 1$ (IN 1024 STEPS)

GN_2 VALVE - $\dot{m}_g = k_g \frac{P}{\sqrt{T}} A_g = 21.8 \frac{P}{\sqrt{T}} A_g \quad P > 1.5$

$= 21.8 \frac{P}{\sqrt{T}} \left(2 - \left[\frac{1.5}{P}\right]^{1.7} \right) A_g \quad 1 \le P \le 1.5$ $\quad 0 \le A_g \le 1$ (IN 256 STEPS)

TEMPERATURE SENSOR $\frac{1}{1 + t_1 s}$ WHERE $t_1 = \frac{1}{2}$ TO 3 secs

PRESSURE SENSOR $\frac{1}{1 + t_2 s}$ WHERE $t_2 = \frac{1}{4}$ secs

FAN DYNAMICS $\frac{N}{N_{SET}} = \frac{5}{s^2 + 2.8 s + 5}$

Figure 6 concluded.

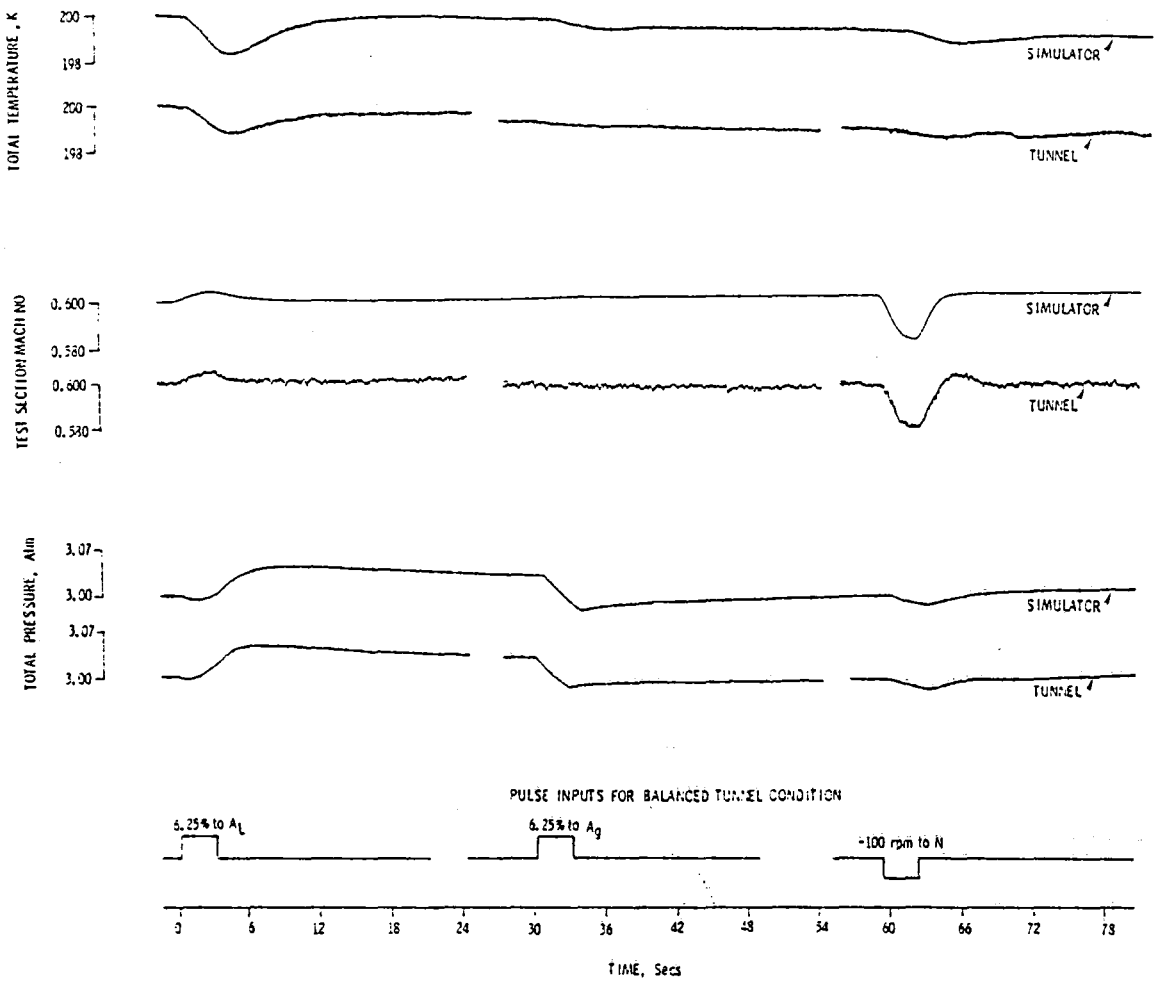

Figure 7. Simulator and tunnel transient response data at T = 200 K, M = 0.6, and P = 3 atm.

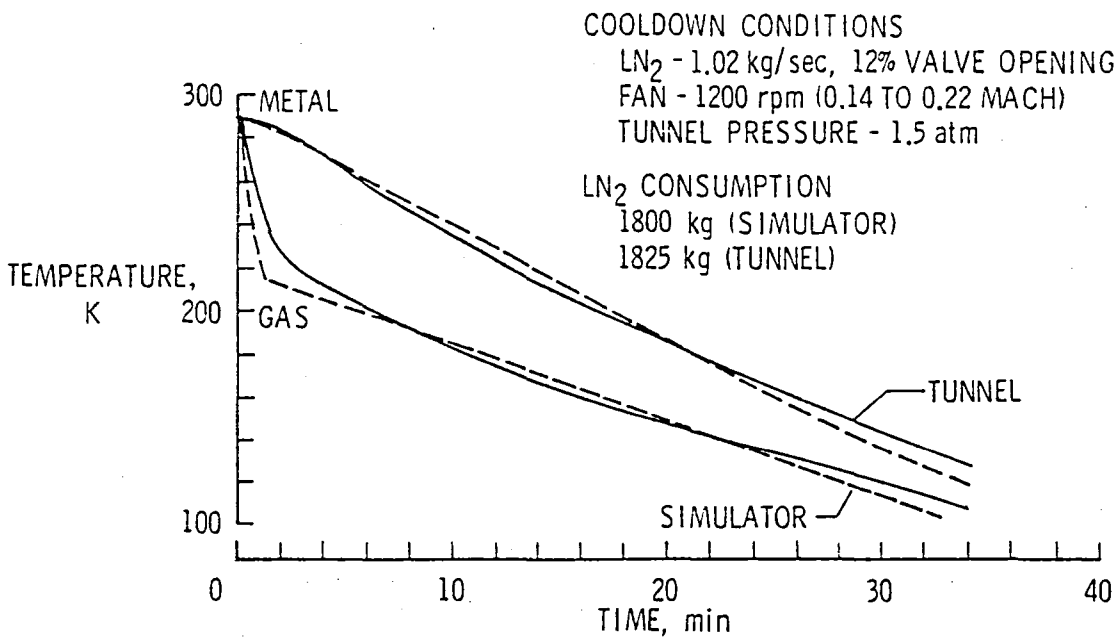

Figure 8. Cool-down profile for tunnel and simulator.

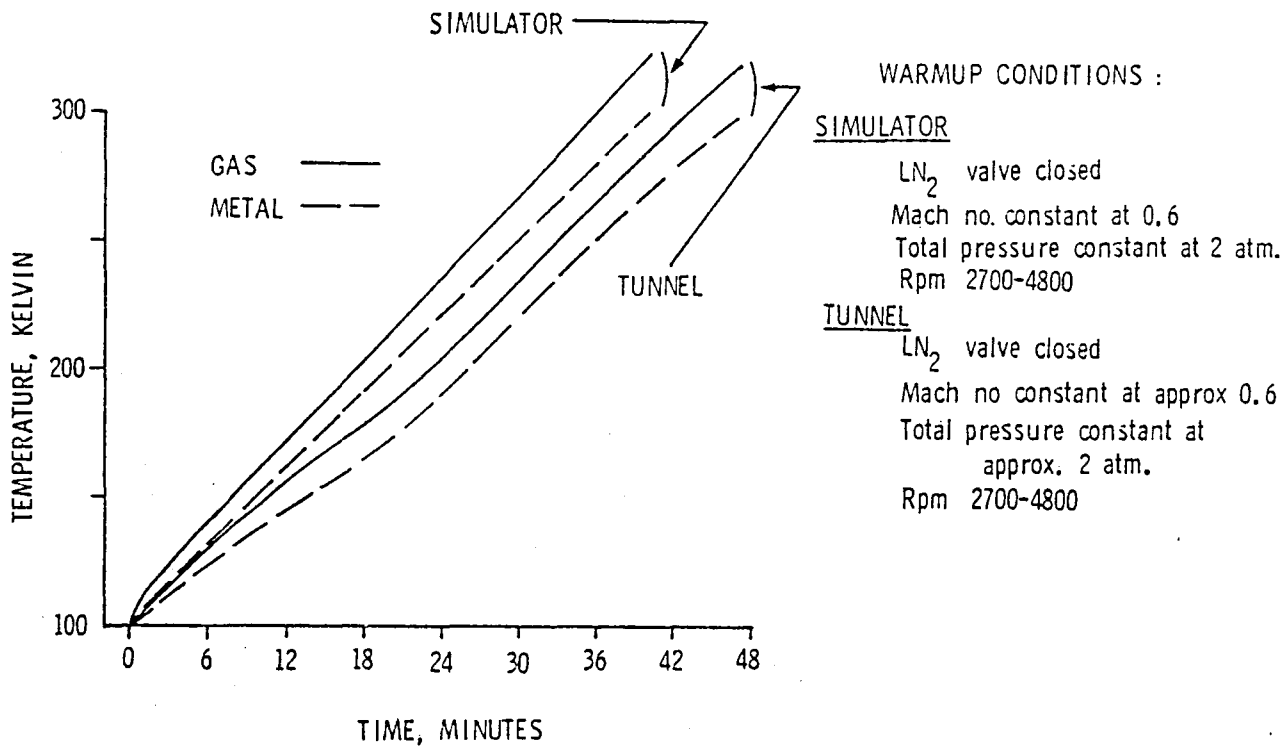

Figure 9. Comparison of tunnel and simulator warmup profiles.

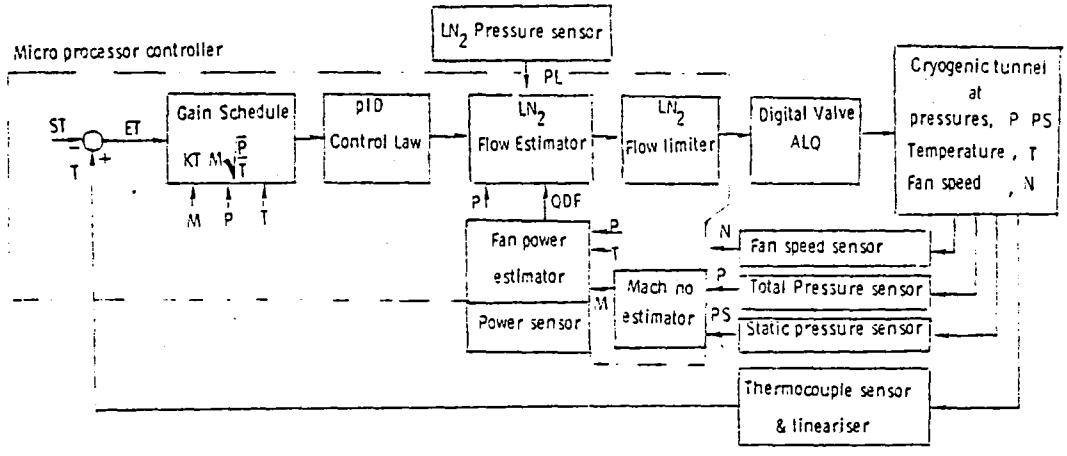

Control law

$$ET = T - ST$$

$$ALQ = \left\{ \frac{M \cdot \sqrt{P} \cdot KT}{KL \cdot \sqrt{T}} \left(pT \cdot ET + IT \cdot \int ET + DT \cdot \frac{d}{dt} ET \right) + KB \cdot FF \right\}$$

IF $ALQ > MAX$; $ALQ = MAX$ IF $ALQ < MAX$; $ALQ = ALQ$

$$KB = \frac{QDF}{(121+T) \cdot KL} \qquad QDF = \frac{KF \cdot P \cdot \sqrt{T} \cdot M^3}{(1 + 0.2 \cdot M^2)^3}$$

$$MAX = \left(KB \cdot FF + \frac{255 \cdot P \cdot V \cdot TGR}{T \cdot (121+T) \cdot KL} \right) \cdot (1-LLT) + LLT$$

Logic

IF $ET > 0$; $FF = 1$ IF $ET < -5$; $FF = 0$

IF $ET < 5$; $LLT = 1$ IF $ET > 10$; $LLT = 0$

Figure 10. Automatic temperature control scheme for 0.3-m TCT.

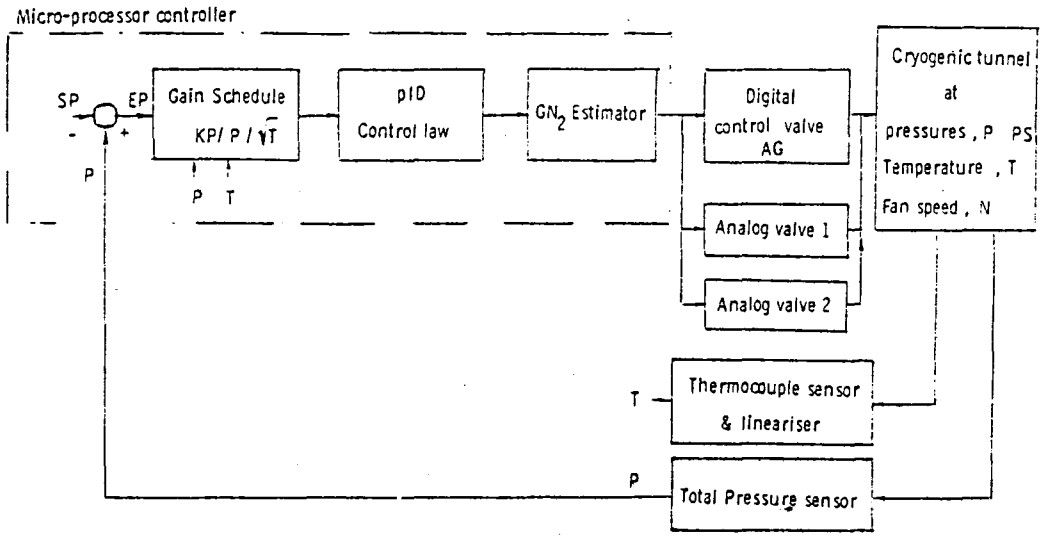

Control law

$$EP = P - SP$$

$$AG = \frac{KP}{KG\, P\sqrt{T}} \left[DP \cdot EP + IP \int EP + DP \cdot \frac{d}{dt} EP \right]$$

Logic

$SUM = 0$ $\quad SUM_{past} =$ SUM, UA seconds ago

IF $AG > 0.9$: $SUM = SUM_{past} + 0.125$

IF $AG < 0.5$: $SUM = SUM_{past} - 0.125$

IF $SUM < 1$: $A1 = SUM$ $\quad A2 = 0$

IF $SUM > 1$: $A1 = 1.0$ $\quad A2 = SUM - 1$

Figure 11. Automatic pressure control scheme for 0.3-m TCT.

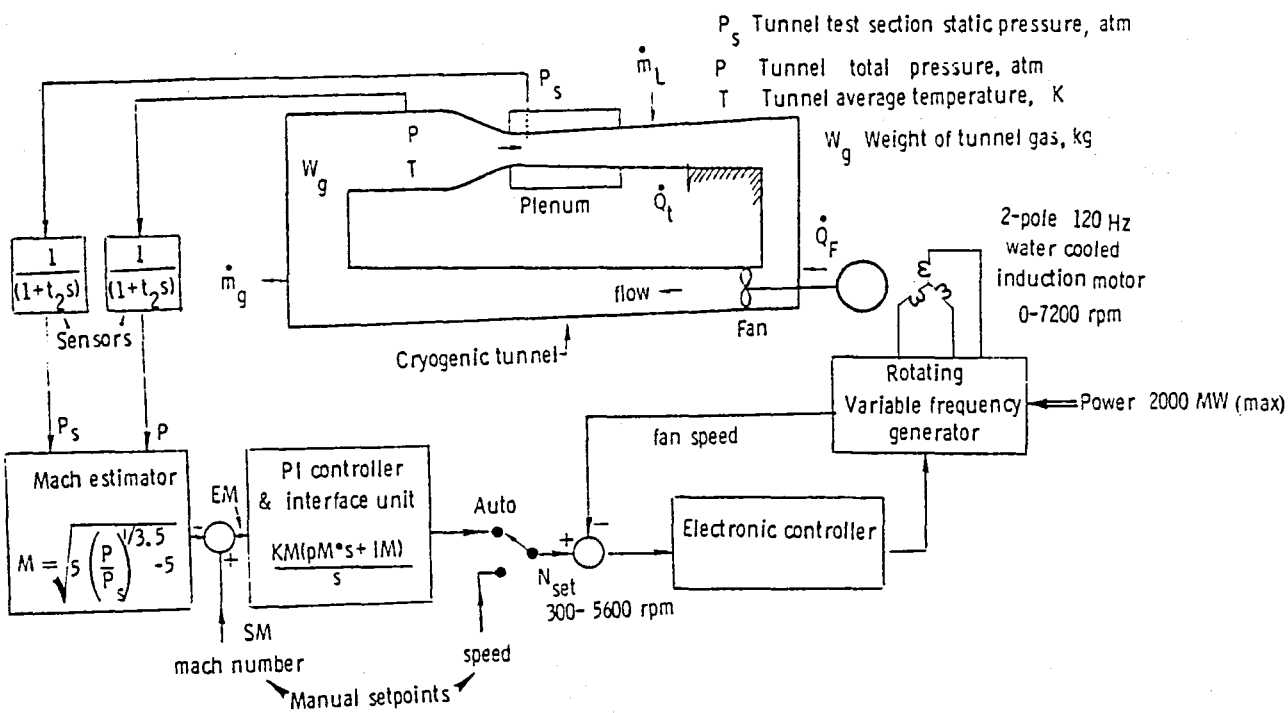

Figure 12. Automatic Mach number control scheme for 0.3-m TCT.

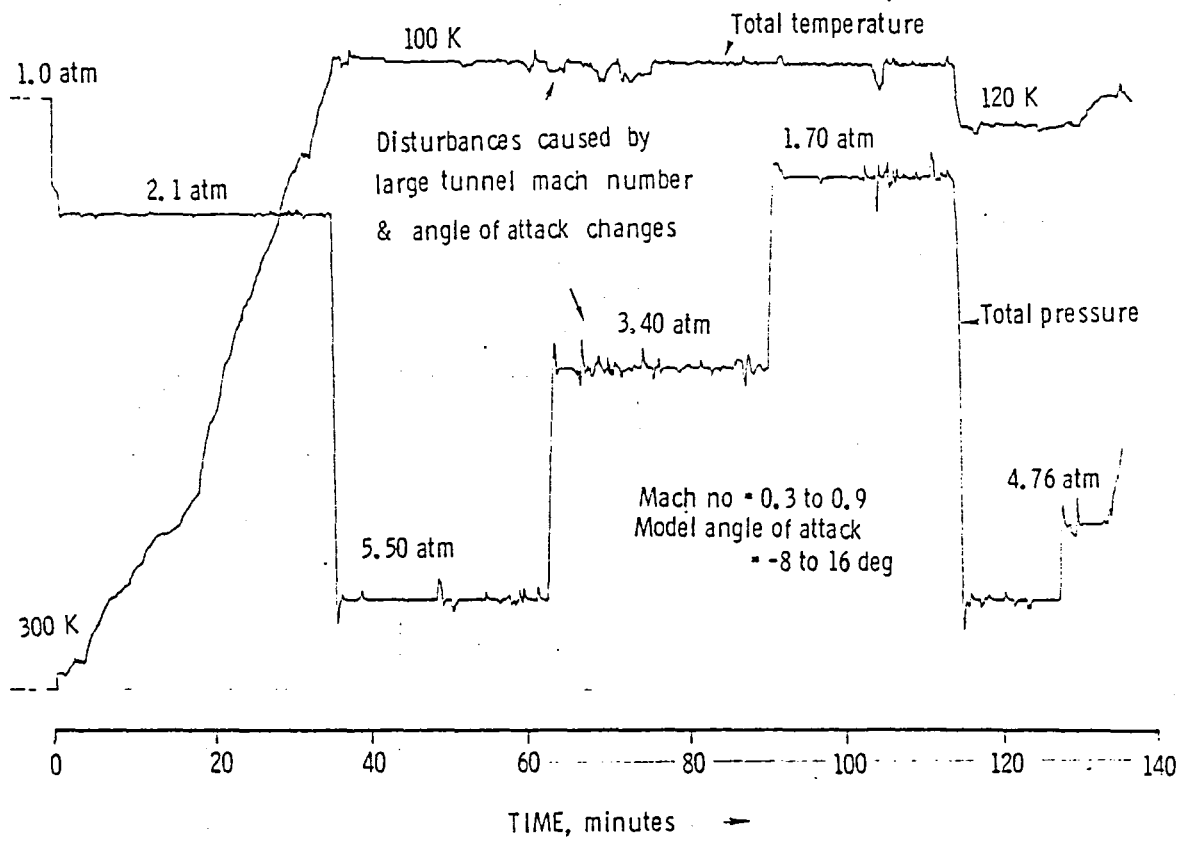

Figure 13. Typical 0.3-m TCT test with temperature and pressure on automatic control.

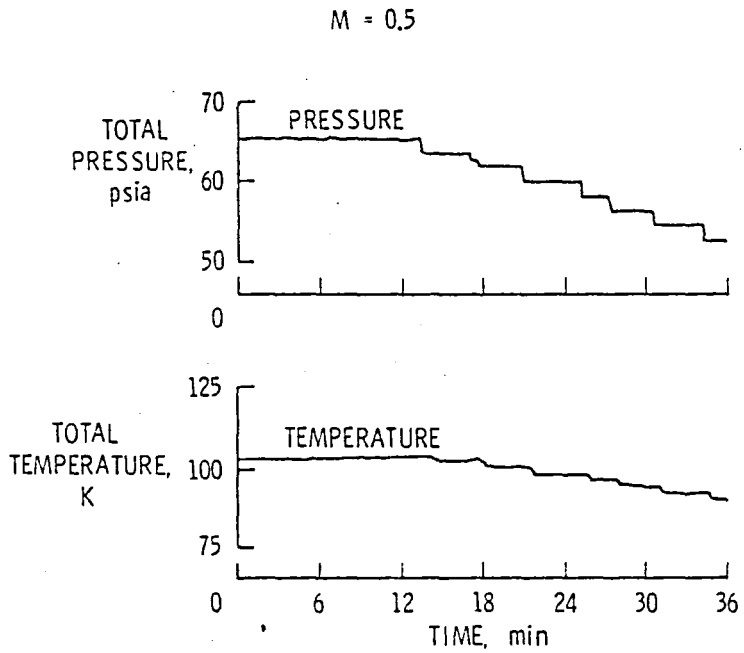

Figure 14. Typical 0.3-m TCT test temperature and pressure on automatic control.

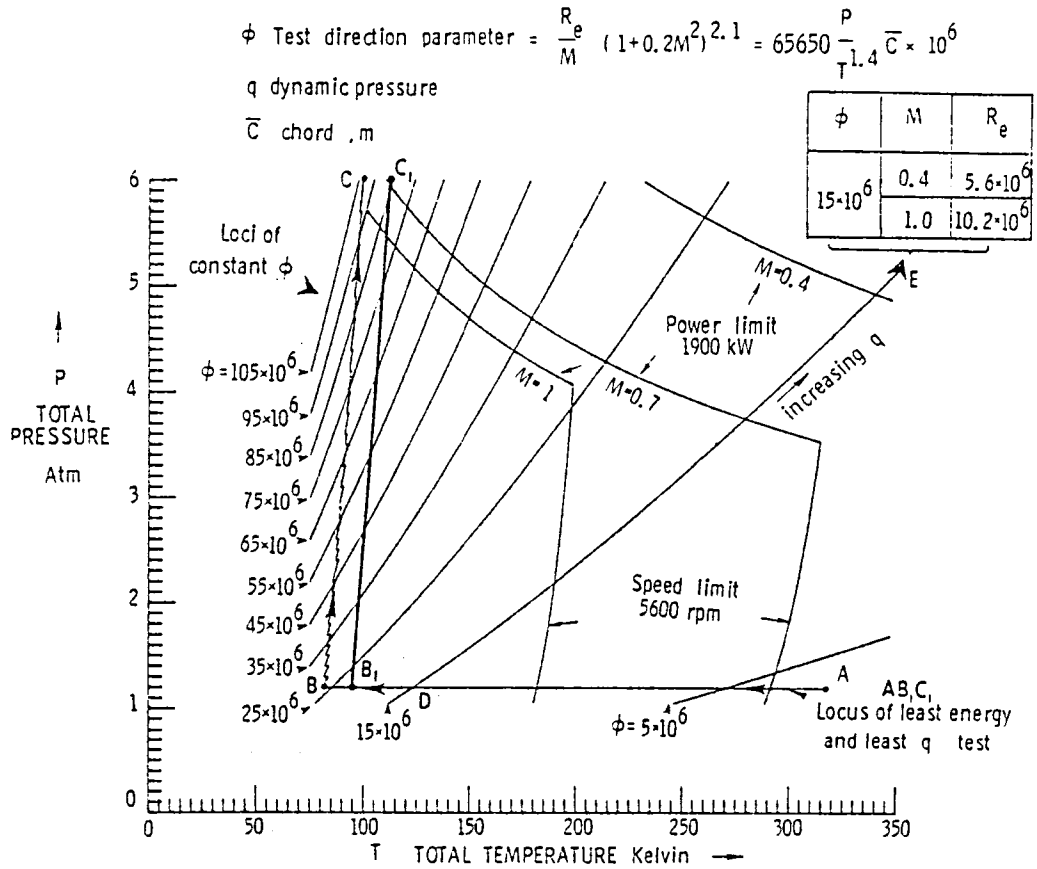

Figure 15. Test direction design in cryogenic wind tunnels—locus of least liquid nitrogen consumption and least q in P-T plane.

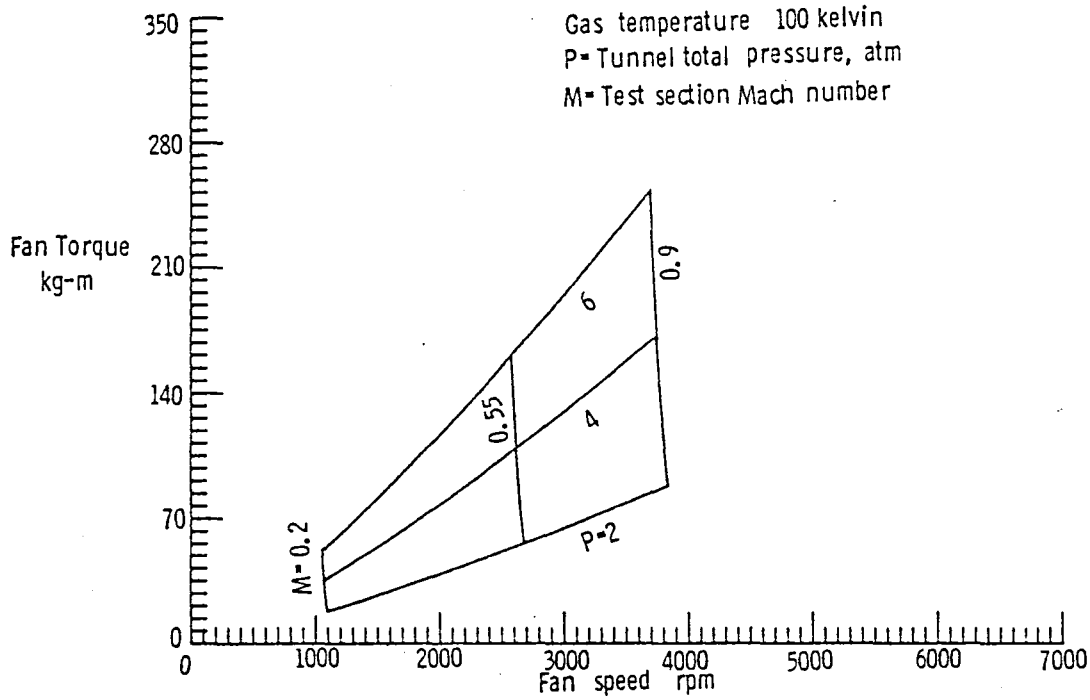

Figure 16. Speed torque characteristics of 0.3-m TCT fan load, 100 K.

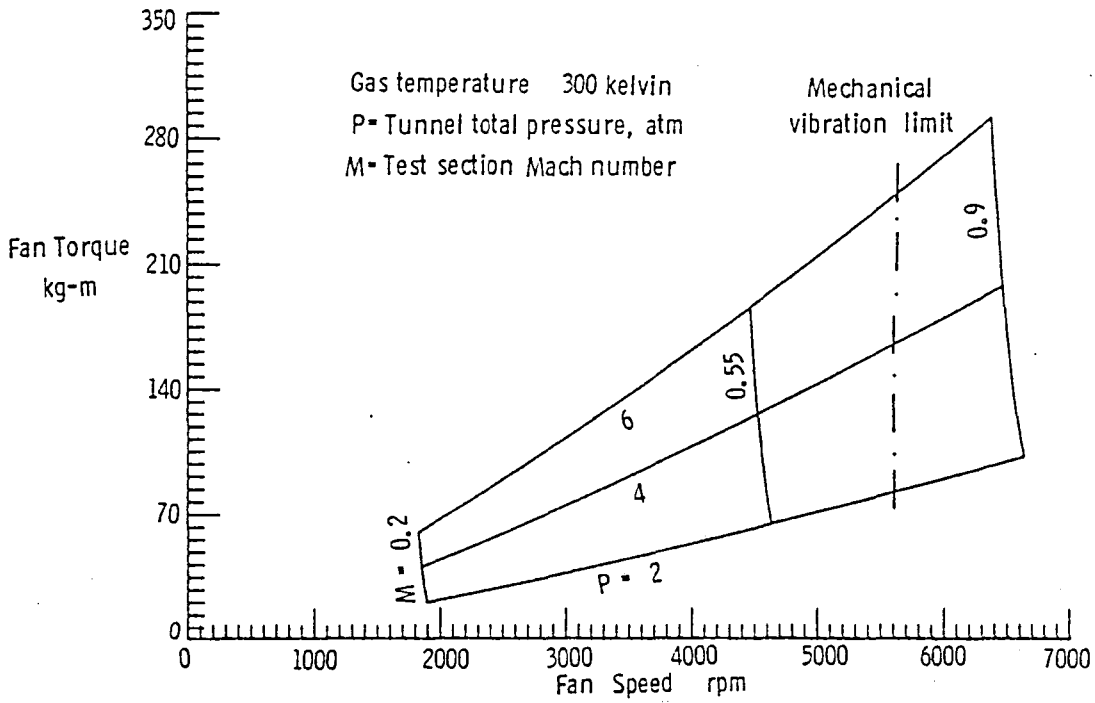

Figure 17. Speed torque characteristics of 0.3-m TCT fan load, 300 K.

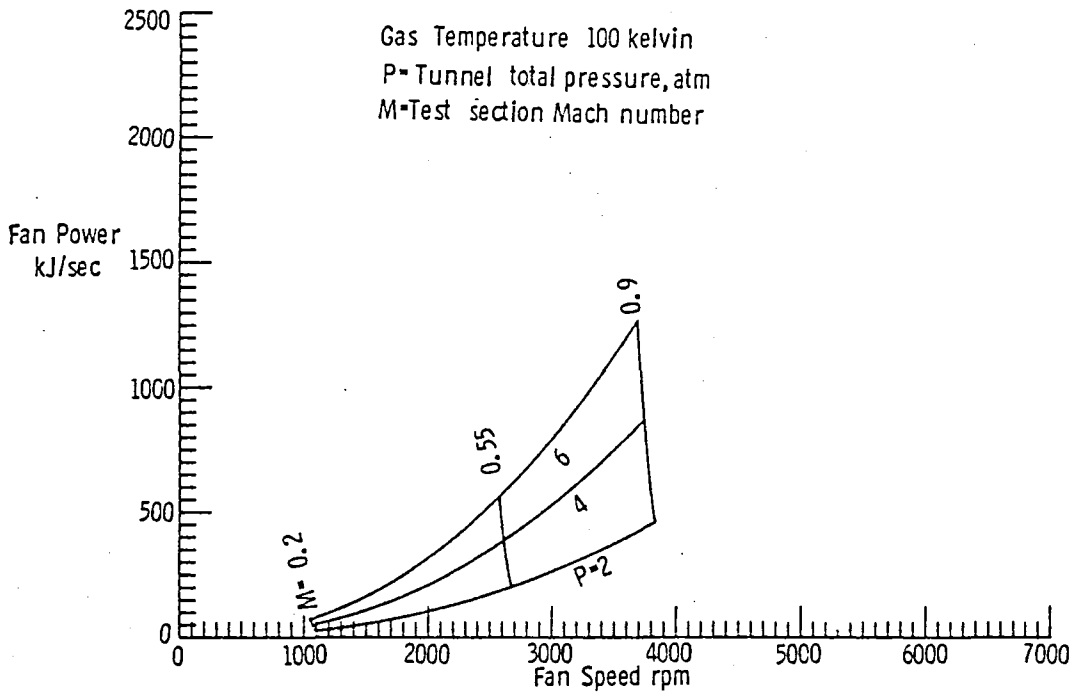

Figure 18. Speed power characteristics of 0.3-m TCT fan load, 100 K.

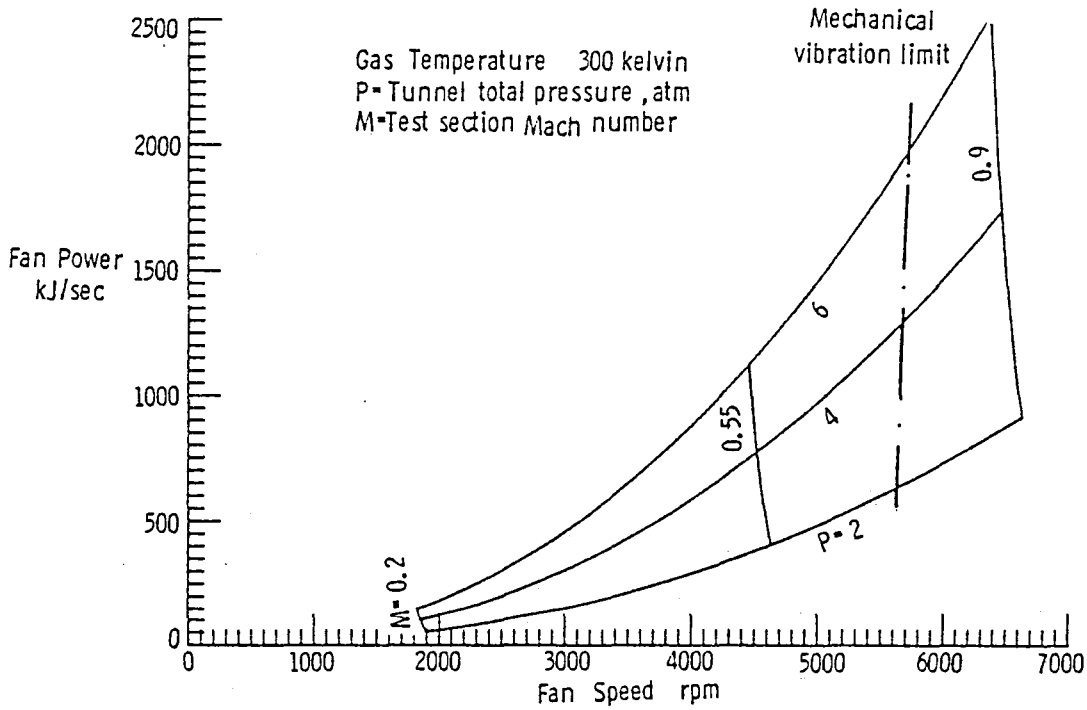

Figure 19. Speed power characteristics of 0.3-m TCT fan load, 300 K.

End of Document